Old Dominion University
ODU Digital Commons

CCPO Publications | Center for Coastal Physical Oceanography

2021

Dynamical Downscaling Projections of Late 21st Century U.S. Landfalling Hurricane Activity

Thomas R. Knutson

Joseph J. Sirutis

Morris A. Bender

Robert E. Tuleya
Old Dominion University, rtuleya@odu.edu

Follow this and additional works at: https://digitalcommons.odu.edu/ccpo_pubs

 Part of the Climate Commons, and the Oceanography Commons

Original Publication Citation

Knutson, T. R., Sirutis, J., J., Bender, M. A., & Tuleya, R. E. (2021). *Dynamical downscaling projections of late 21st century U.S. landfalling hurricane activity*. Research Square, 1-11. https://doi.org/10.21203/rs.3.rs-806601/v1

This Article is brought to you for free and open access by the Center for Coastal Physical Oceanography at ODU Digital Commons. It has been accepted for inclusion in CCPO Publications by an authorized administrator of ODU Digital Commons. For more information, please contact digitalcommons@odu.edu.

Research Square

Preprints are preliminary reports that have not undergone peer review.
They should not be considered conclusive, used to inform clinical practice,
or referenced by the media as validated information.

Dynamical Downscaling Projections of Late 21st Century U.S. Landfalling Hurricane Activity

Thomas R Knutson (Tom.Knutson@noaa.gov)
GFDL/NOAA https://orcid.org/0000-0003-4541-519X
Joseph J. Sirutis
Deceased
Morris A. Bender
Princeton University
Robert E. Tuleya
Old Dominion University

Research Article

Keywords: CMIP3, GFDL hurricane model, CMIP5 modeled, tropical cyclone, Landfalling hurricane

Posted Date: September 7th, 2021

DOI: https://doi.org/10.21203/rs.3.rs-806601/v1

License: This work is licensed under a Creative Commons Attribution 4.0 International License. Read Full License

Abstract

U.S. landfalling tropical cyclone (TC) activity was projected for late 21st century conditions using a two-step dynamical downscaling framework. A regional atmospheric model, run for 27 seasons, generated tropical storm cases. Each storm case was re-simulated (up to 15 days) using the higher resolution GFDL hurricane model. Thirteen CMIP3 or CMIP5 modeled climate change projections were explored as scenarios. Robustness of projections was assessed using statistical significance tests and comparing the sign of changes derived from different models. The proportion of TCs (tropical storms and hurricanes) making U.S. landfall increases for the warming scenarios (by order 50% or more). For category 1-3 hurricane frequency, a robust decrease is projected (basin-wide), but robust changes are not projected for U.S. landfalling cases. A relatively robust increase in U.S. landfalling category 4-5 hurricane frequency is projected, averaging about +400% across the models; 10 of 13 models/ensembles project an increase (statistically significant in three individual models), while three models projected no change. The most robust projections overall for U.S. landfalling TC activity are for increased near-storm rainfall rates: these increases average +18% (all tropical storms and hurricanes), +26% (all hurricanes), and +37% (major hurricanes). Landfalling hurricane wind speed intensities show no robust signal, in contrast to a ~5% increase in basin-averaged TC intensity; basin-wide Power Dissipation Index (PDI) is projected to decrease, partly due to decreased duration. TC translation speed increases a few percent in most simulations. A caveat is the framework's low correlation of modeled U.S. TC landfalls vs. observed interannual variations (1980-2016).

1. Introduction

U.S. landfalling TCs (hurricanes and tropical storms) can cause major damage to coastal and inland infrastructure, and it is of great interest to better understand how landfallling TC activity may change under future anthropogenic climate change, with a particular focus on landfalling hurricanes. Relatively long records (since at least about 1900) are available for tropical storm, hurricane, and major hurricane landfalls (e.g., Vecchi and Knutson 2008, 2011; Klotzbach et al. 2020; Vecchi et al. 2021), but these time series do not show any significant increases since 1900. The lack of a significant change in long TC landfalling records is in contrast to the case for global mean temperature, where a clear anthropogenic warming signal has been identified (IPCC AR5). This indicates that TC landfall frequency in the above regions is clearly not a metric with a strongly detectable anthropogenic signal even on a century time-scale. A previously published Atlantic-basin-focused dynamical downscaling study (Knutson et al. 2013, hereafter K13) addressed the potential impact of future global warming on TCs, but the previous study focused on lifetime maximum intensities of TCs, by using five-day high-resolution simulations of storms near their times of maximum intensity. Importantly, K13 did not focus on the U.S. landfalling stages, which often were outside of the 5-day window simulated with the high resolution model. The purpose of the present study is to revisit the two-step dynamical downscaling study of K13, with a specific purpose of focusing on the U.S. landfalling stages of the simulated hurricanes (for the Contiguous U.S., i.e., excluding Hawaii, Puerto Rico, Guam, etc.). Through this study, we aim to provide more societally relevant information about the damage potential impacts of the storms (in terms of intensity, frequency, rainfall) under various climate change scenarios. Previous studies on possible future changes in U.S. landfalling TCs have reported model projections of: reduced probability of TC landfall over the southeastern U.S. and increased probability over the northeastern U.S. (Murakami and Wang (2010); reduced TC occurrence over the southern Gulf of Mexico and Caribbean (Colbert et al. 2013); increased average TC rain rates over U.S. land regions (Wright et al. 2015); and increased likelihood of faster-moving landfalling TCs in the Texas region (Hassanzadeh et al., 2020). The latter study result is qualitatively in contrast to an observed finding for historical TC of a significant reduction in propagation speed over the U.S. land regions since 1900 (Kossin 2019) —an observed result which was not reproduced in a historical forcing model simulation (Zhang et al. 2020). Levin and Murakami (2019) found that historical increases in anthropogenic climate forcing led (qualitatively) to increased frequency of U.S. major hurricane landfall in their model, although a significant increase in U.S. major hurricane frequency is not seen in observations since 1900 (Klotzbach et al. 2020) or since the late 19th century (Vecchi et al. 2021).

Our study explores 21st century climate change projections for U.S. landfalling hurricane activity using a two-step dynamical downscaling framework, together with tropical climate change projections from multiple CMIP3 and CMIP5 climate models– the same models as used in K13. In the earlier study, the highest resolution simulations with the GFDL hurricane model (i.e., the second step of our two-step downscaling procedure) were limited to five days in length, as we were closely following the procedures of the operational GFDL hurricane model from that time period, which had some operational limitations. Given this five-day limitation of simulation length in K13, the focus of the high-resolution simulations was on the time period in which each hurricane was approaching its maximum intensity. Specifically, in K13 each five-day downscaling case was started from initial conditions, obtained from the 18 km grid Zetac regional atmospheric model (Knutson et al. 2007; hereafter K07), beginning two days prior to the storm's time of maximum intensity as simulated in the Zetac model. The Zetac model simulated hurricanes only up to about 50 m s-1 intensity in terms of surface wind speed, which was one reason why the second downscaling step with the higher-resolution (9 km spacing for the inner grid) was necessary. In contrast, in the present study, where we wish to focus on the landfalling stages as well as simulate realistic storm intensity and structure throughout each storm's life cycle, we start each high-resolution hurricane model simulation (storm case) using initial conditions from the regional Zetac model at the time when tropical storm intensity of 17.5 m s-1 is first reached in the Zetac model, and then integrate the hurricane model forward for 15 days. More details of methodology are provided in Sect. 2, results of the experiments are presented in Sect. 3, and our summary and conclusions in Sect. 4.

2. Methodology

The methodology for our study mostly follows that in K13, K07, and Bender et al. (2010), and is described in detail in those studies. Here the methodology is presented only in abbreviated form here, where we focus mainly on aspects of methodology that differ from K13 and K07. The reader is referred to these previous studies for further details.

2.1. Present-day hurricane simulations

The simulation of Atlantic hurricanes proceeds in in several stages. Before we perform climate change simulations, we first want to assess whether our complete modeling system is able to adequately simulate Atlantic hurricane activity for a given set of environmental conditions. To explore this, we first test

our system on present-day large-scale climate as defined by the time-evolving NCEP/NCAR Reanalysis I (Kalnay et al. 1996) of the atmosphere and observed sea surface temperature (SST) evolution for 1980–2016. For each year (1980–2016), we simulate the three-month period August-October with the regional 18-km grid Zetac regional model, using the reanalysis to provide lateral boundary conditions, the atmospheric initial conditions, and the time-evolving target fields for interior spectral nudging of the very large scale (zonal and meridional wavenumber 0–2 of the regional domain) atmospheric environment, with a nudging timescale of 12 hours. The simulations were limited to the peak three months of the Atlantic TC season (Aug. – Oct.) to save on computation requirements, which may introduce some uncertainty to our results, particularly if aspects of seasonality, such as the length of the Atlantic TC season, were to change with climate warming. For example, Dwyer et al. (2015) find that in model projections, models that project fewer TCs with climate warming also simulate shorter seasons, and vice versa for models projecting more TCs. This potential limitation of our Aug.-Oct. season approach should be kept in mind in interpreting our results. The model was run over specified time-evolving SSTs. The Zetac regional model is a nonhydrostatic model run here without convective parameterization (see K07 for details).

Tropical storm cases are identified in these three-month simulations using the automated procedure described in K07, including a requirement for warm-core structure, surface wind speeds for the storm feature of at least 17.5 m s-1, and total duration of at least 48 hours (not necessarily consecutive hours) at an intensity of at least 17.5 m s-1. Landfalling TCs for the Contiguous U.S. (CONUS) were defined by the intersection of the surface center of the TC (defined by the minimum in surface pressure) with the coastline (https://www.nhc.noaa.gov/aboutgloss.shtml), where the land region was part of the 48 contiguous states (excluding Alaska and Hawaii). Multiple CONUS landfalls by a single storm were counted as separate landfalls in our statistics.

Each individual tropical storm case from the Zetac regional model is then re-run as an individual 15-day case study using the GFDL Hurricane Model. The GFDL Hurricane Model has been used operationally by the National Weather Service (NWS) since 1995 (Bender et al. 2007; 2010) until it was retired from operations in 2017. The version used in this study was the model used in Bender et al. (2010), which was the version that was operational from 2006 through 2010. The model is a triply nested moveable mesh model designed for hurricane track and intensity prediction, and has grid-spacing of about 8.5 km in the innermost 5ox5o nest. The hurricane model has been coupled to the Princeton Ocean Model since 2001 (Bender et al. 2007) and for the present-day simulations uses a realistic present-day (U.S. Navy GDEM, or Generalized Digital Environmental Model) climatology of ocean subsurface temperature and salinity so that the hurricane model is able to accurately simulate the ocean response to the strong hurricane forcing and generate a realistic “cold wake” as it passes over the ocean (Bender et al. 2007). Following the procedure used operationally (2006–2010) for storm initialization, the ocean model state for each storm case is initialized by running the ocean model for two days using the GDEM climatology values for ocean temperature and salinity with SSTs prescribed. During this first step, a sharpening technique is employed in order to assimilate a reasonable climatologically based Loop Current and Gulf Stream ocean structure (Yablonsky et al. 2015). Next, starting three days prior to the storm case start date, atmospheric forcing is imposed, based on the model’s storm wind field. In this second step, the SSTs as well as ocean temperatures and salinity are allowed to evolve. This procedure is used to initialize a cold wake in the SST and ocean temperature field due to the passage of the storm. A limitation of the version of the operational GFDL Hurricane Modeling System used in this study was that the dynamical ocean domain did not cover the full North Atlantic basin but rather the coupled model used two separate ocean model domains—one covering the central to eastern Atlantic and the other the central to western Atlantic (see Fig. 5 of Bender et al. 2007). Storms traversing the central Atlantic could run off one of these grids and lose their ocean coupling. However since the two ocean grids overlapped when this occurred, we restarted the storm on the second ocean grid before the coupling was lost and continued the simulation with full ocean coupling until landfall. Since this happened only for a small subset of runs, and the transition occurred very far from U.S. landfall, and was treated the same for both present-day and warm climate experiments, we believe that this limitation of our model framework was very unlikely to affect our overall conclusions.

In addition, during the 15-day integrations, the hurricane model atmosphere tended to drift toward the model’s climatological state, which differs from that of the host (Zetac) regional model and NCEP/NCAR Reanalysis. However, the average drift that occurs is found to be similar for present-day climate and future warm climate scenarios, so that any systematic effects of the drift on the storm characteristics should be similar in the present-day and warm climate cases.

Figure 1 compares the tracks and intensities of simulated U.S. landfalling TCs from the Zetac regional model and the GFDL Hurricane Model for the years 1980–2013. The tracks from the higher resolution model resemble those of from the Zetac regional model, although the intensities extend to higher categories (up to category 5) in the hurricane model compared to almost no track segments above category 1 in the Zetac regional model.

One test of the simulation skill of our two-step downscaling model framework is a comparison of the year-to-year variability of August-October observed mean storm counts with that from the modeling framework for different categories of tropical storms and hurricanes (Fig. 2). For example, if the model framework, which was only provided large-scale information about the year-to-year variability of the Atlantic basin SSTs and atmospheric circulation, along with very large-scale interior spectral nudging, is still able to generate useful information about tropical storm, hurricane, and intense hurricane numbers and their year-to-year variation, this increases our confidence that the framework can translate some forms of atmospheric and SST variability into useful information about hurricane activity.

The time series in Fig. 2 show that the model is indeed useful for simulating Atlantic basin hurricane activity given specified large-scale atmospheric, oceanic, and SST conditions. Specifically, with only SSTs, ocean temperature climatology, and time-varying NCEP/NCAR Reanalysis boundary forcing and very large-scale interior domain nudging, the system has the following correlation with observed 37 year time series of Atlantic basin Aug-October storm counts: 1) all TCs (tropical storms and hurricanes): r = 0.77 (explained variance: 59%); 2) Category 1–5 hurricanes: r = 0.68 (explained variance: 46%); 3) major (Category 3–5) hurricanes: r = 0.56 (explained variance: 31%); 4) very intense (Category 4–5) hurricanes: r = 0.31 (explained variance: 10%). Assuming independent years, correlations above 0.329 are significant at the 0.05 level, so for all cases except Category 4–5 hurricanes the results show significant correlation. For the Category 4–5 hurricanes, the results are nearly statistically significant.

We note that there are rising trends evident in many of the time series in Fig. 2. The modeled trends are similar to the observed with the notable exception of basin-wide hurricane frequency (Fig. 2c) where the model has a more rapid rising trend than observed. The cause of these rising trends in observations

remains a topic of research, as the time period (1980–2013) is relatively short for detection of greenhouse gas warming influence, and since both internal variability and changes in aerosol forcing are possible contributors to such TC-related trends (e.g., Goldenberg et al. 2001, Mann and Emanuel 2006; Zhang et al. 2013, Dunstone et al. 2013, Vecchi et al. 2017, Yan et al. 2017, Murakami et al. 2020; Bhatia et al. 2018). Our simulations indicate only that changes in the large-scale environment (including SSTs) help to explain the rising trends in observed TC and hurricane frequency but do not elucidate the causes of the environmental changes. However, we expect that the observed Atlantic hurricane frequency trends, and tropical Atlantic SST changes, since 1980 have multiple causes and several studies suggest the TC frequency increases are likely not primarily a response to increasing greenhouse gases alone. Thus, the over-prediction of the observed trend in hurricane frequency (1980–2013) evident in our model framework does not invalidate its potential use for greenhouse gas-driven future warming scenarios.

The model framework's performance is much less skillful for U.S. landfalling storm counts. None of the simulated time series of storm count are significantly correlated with observed variations: 1) all TCs: r = 0.21 (explained variance: 4%); 2) Category 1–5 hurricanes: r = 0.15 (explained variance: 2%); 3) major (Category 3–5) hurricanes: r=-0.07 (no explained variance).

The above results provide an important caveat to our study. While the two-step model framework is relatively skillful at reproducing the year-to-year variation of basin-wide tropical storm and hurricane counts, this skill does not carry through to U.S. landfalling counts. Thus, while the basin-wide results provide model-based evidence that the year-to-year variability in the basin-wide numbers is not random "weather noise" but rather is controlled to a large extent by large-scale environmental conditions, the U.S. landfalling count variations seem much more difficult to capture using our modeling framework. While we are not aware of many other modeling systems that can successfully simulate U.S. landfalling TC frequency, one exception is the HiFLOR model (Murakami et al. 2016), which does show some skill in predicting seasonal U.S. landfalling TC frequency over the period 1980–2015, suggesting that there are large-scale controls on this metric that are not being well-captured in our two-step model framework. We have chosen to use our modeling framework to explore future U.S. landfalling behavior under global warming to take advantage of its high-resolution for simulating hurricane structure, while keeping in mind the model's limitations for reproducing observed interannual variations of TC frequency from large-scale interannual variations of environmental conditions.

2.2. Climate Change Downscaling Experiments

Following on the 37 Atlantic hurricane seasons of present-day two-step downscaling simulations (1980–2016), we perform similar experiments, but applying a set of climate change conditions, for 27 of the 37 present-day seasons (1980–2006).

We first create a series of climate change "delta" fields, which we can add to the NCEP/NCAR Reanalysis, to create a series of warm-climate perturbation experiments that use realistic conditions (i.e., the reanalysis) as the baseline case. Specifically, we use we use changes in SST, sea level pressure (SLP), air temperature, relative humidity, and wind velocity to modify the NCEP/NCAR reanalysis fields that are used as boundary forcing and as the nudging target for the interior spectral nudging procedure with the Zetac regional model. As described in K13, for CMIP3 models, these perturbations included an 18-model ensemble average perturbation (models listed in K13), which was the August-October average of 2081–2100 minus 2001–2020 for the Special Report on Emission Scenarios A1B (SRES A1B) scenario. Then for 10 of the 18 CMIP3 models (identified later in this report), we created individual model perturbation fields by computing the linear trend of each model's data for 2001–2100 then computing the 2081–2100 minus 2001–2020 difference of the data projected onto the linear trend. Our experimental design uses the interannual variability from the NCEP/NCAR Reanalysis, which assumes that the interannual variability of these fields does not change with climate change. Projected changes in interannual variability of these fields are generally assessed as having less confidence than changes in the large-scale time-mean environmental fields, although this adds some additional uncertainty to our TC projections. We constructed two 18-model ensemble mean CMIP5 model warm climate scenarios using the 2016–2035 (early 21st century) or 2081–2100 (late 21st century) period of the CMIP5 RCP4.5 scenario versus the baseline period of 1986–2005 of the CMIP5 historical runs (see K13 for a list of the models). The global temperature difference between present-day and the warm-climate condition was 1.69oC for CMIP3 vs. 1.70oC for the CMIP5 late-21st century case. In sensitivity experiments, we found that hurricane model intensity changes in the warm climate scenarios were relatively insensitive to the small increase in the ocean subsurface vertical temperature gradients associated with the SST warming scenarios (see also Tuleya et al. 2016). Therefore, following Knutson et al. (2013) for the ocean subsurface temperature profiles in the warm climate runs, we used the 18-model average three-dimensional ocean structure change from the CMIP3 models to represent the change in ocean temperature stratification in the warmer climate for all of the hurricane model climate change experiments.

3. Results Of Climate Change Downscaling Experiments

In this section, we examine the results of our climate change downscaling experiments. In the discussion below, we refer to the 13 sets of experiments as 13 "models", even though these are really the downscaling results based on input climate change signals from a particular model, or in some cases based on the ensemble mean climate change signal from a collection of models (18 CMIP3 models, and 18 CMIP5 models for the early 21st century or late 21st century scenarios).

There are many TC metrics that can be examined in our 13 different sets of experiments. To focus on results from our experiments that are relatively more robust, we present the results in a summary form showing both the level of agreement across the models for projected changes for various metrics, along with statistical significance tests for individual models. The statistical tests assume the 27 separate seasons (years) are independent samples. Using this summary approach, Table 1 examines two distinct but important sources of uncertainty in projections: modeling uncertainty as indicated by the agreement in sign of the projected change for the 13 different models, and internal variability uncertainty, as estimated by statistical significance testing on the 27 different samples (years) from each model (with significant changes being bold and underlined). Table 1 presents a summary of the experimental results in a way that these two different sources of uncertainty can be assessed, for both U.S. landfalling TCs (at the time of landfall) and the basin-wide results. The basin-wide results are based on either the time of maximum storm wind speed intensity or on the entire lifecycle of each TC in each year for the case of accumulated activity metrics like the PDI (Power Dissipation Index).

Table 1 indicates that a very robust signal emerges for increasing TC rainfall rates, for all (basin-wide) TCs (in Table 1, see rows labeled: rain_all_TC (cat 0–5), rain_hur_(cat 1–5), rain_mhur (cat 3–5), rain_hur45) and to a lesser degree (in terms of statistical significance) for U.S. landfalling TCs (in Table 1: lf_rain_all_TC (0–5), lf_rain_hur (1–5), lf_rain_mhur (cat 3–5)). The rainfall rates are examined for various categories of TC. Robust increases in rainfall rates are indicated across all TC categories. For basin-wide TCs, the increase is averages about 20% regardless of TC category. Interestingly, for the U.S. landfalling TCs, the percentage increase in TC rain rate with climate warming increases monotonically with storm category, from + 19% averaged over all categories of TC (in Table 1: rain_all_TC (cat 0–5) to almost + 200% for TCs that are Category 4 or 5 at landfall (in Table 1: lf_rain_hur45). The reason for the increased sensitivity of this metric for very intense landfalling TCs is uncertain. There is a strong observed relationship between rainfall rate and intensity at landfall (Tuleya et al., 2007). As will be discussed further below, there is some indication in Table 1 for increased TC intensities with warming (basin-wide) although TC intensity at landfall shows less robust change in the simulations. The increased TC intensity over ocean regions may lead to amplified increased TC rain rates over oceans that may exceed the increase expected from the Clausius-Clapeyron relation (increasing water vapor with warming) alone (e.g., Liu et al. 2019). However it remains unclear why the rain rate percentage increase at landfall is larger for higher category storms (e.g., + 193% for lf_rain_hur45 vs. 18% for lf_rain_all_TC (0–5))—although these are relatively fewer in number than lower-category landfalling storms and thus the statistics may be affected by limited sample sizes. Previous studies that have projected or modeled substantial increases in rain rates for U.S. landfalling TCs include Wright et al. (2015) and Reed et al. (2021). In addition, Patricola and Wehner (2018), Hill and Lackmann (2011) and several other studies reviewed in Knutson et al. (2020) have reported a broadly similar result for precipitation rates of Atlantic TCs in general (while not specifically focusing on the U.S. landfalling stages).

Another relatively robust response seen in the simulations is the prevalence of negative changes (decreases) in the upper 10 rows of Table 1, which concern basin-wide TC frequency changes for various categories of TC. The decreases are particularly robust for basin-wide: category 1 hurricanes (-42%), category 2 hurricanes (-45%), category 3 hurricanes (-43%), all tropical storms and hurricanes combined (category 0–5; -28%), all hurricanes combined (category 1–5; -34%), and major hurricanes (category 3–5; -25%). Basin-wide PDI shows a similarly robust projected decrease of -28%.

The highly significant and robust decreases across models seen for basin-wide frequency of TCs does not carry through very strongly to U.S. landfalling TCs. In particular, the decreases are less robust and significant for the frequency of weaker U.S. landfalling storm classes. On the other hand, a moderately significant and robust increasing signal emerges for U.S. landfalling category 4–5 storms (in Table 1: lf_hur45, average change + 390% with at least nominal increases for 10 of 13 models, no change for the remaining three models, and statistically significant increases for three of the 13 models). This is noteworthy because these storms have historically caused enormous damage upon landfall. In particular, Pielke et al. (2008) found that U.S. landfalling category 4–5 TCs have historically accounted for almost 50% of normalized TC damage in the U.S., despite representing only 6% of historical TC occurrences. As a sensitivity test, we have assessed U.S. landfalling category 4–5 frequency based on surface pressure, rather the surface wind speed criteria (not shown). The statistical test results are similar though slightly less robust than for the wind speed-based results shown in Table 1.

Maximum lifetime TC intensity (in Table 1, max_wind_all_TC; max_wind_hur) is a metric which models have consistently projected to increase with climate warming (Knutson et al. 2020). The results from our experiments are less compelling for simulated U.S. landfalling TCs. For U.S. landfalling hurricanes (in Table 1: lf_maxwnd_hur), intensity at landfall increases at least nominally for about half the models (seven of 13), and in only one of 13 is the change statistically significant. For intensity of U.S. landfalling tropical storms and hurricanes combined (lf_maxwnd_all_TC) no increase of intensity is evident. For basin-wide hurricane intensity (i.e., in Table 1: max_wind_hur, sampling each hurricane's lifetime maximum intensity), the average intensity of hurricanes increases in 12 of 13 models, of which six of the models yield statistically significant increases. The one exception is the downscaling of the CMIP3 HadGEM1 model, which simulates a significant decrease. As discussed in K13, this particular climate model exhibits a greatly enhanced warming in the upper tropical troposphere (Atlantic main development region, 300 hPa) compared to its surface warming—a factor of 3.5 greater, which much more than the average upper tropospheric warming amplification factor of 1.9 to 2.7 in the other CMIP3 models. Amplified upper tropospheric warming compared to the surface is a known detrimental factor for TC intensification in the GFDL Hurricane model (Tuleya et al. 2016). The average TC intensity change across the 13 models is about 5%. This result is relatively consistent with other high-resolution modeling studies (Knutson et al. 2020). Interestingly, this increasing signal is absent if one includes weaker (tropical storm-strength TCs) in the sample, but we consider the hurricane intensity result as the more relevant one for potential climate impacts. In summary, despite the increase in basin-wide hurricane intensity, the average intensity of landfalling hurricanes shows little significant change, nominally averaging about + 2%.

Table 1 shows that the projected average TC duration has a clear tendency to decrease by about 13% (decreasing in 12 of 13 models, with 8 of 13 models projecting a significant decrease). Projected changes in TC translation speed (basin-wide average, labeled "trans_speed" in Table 1) show a weak tendency for an increase across the models, with 10 models projecting an increase (two are significant) and three models projecting a decrease. The slight speed-up of translation speed may be one factor for the tendency for a decrease in duration, as the lifecycle of the storm over a given track would be shortened by the faster propagation speed. However, we have not diagnosed the reasons for the decreased duration in detail.

The proportion of TCs making U.S. landfall tends to increase in the projections according to most, but not all models. For example, Table 1 (U.S. Landfall proportions section, last nine rows of table) indicates that the proportion of all tropical storms and hurricanes that make landfall (labeled "all_TC (cat 0–5)") increases on average by about 50% above its baseline (control run) value of 0.17. Some increase was simulated in all 13 models. For all hurricanes, the proportion making U.S. landfall (labeled "hur (cat 1–5)") is projected to increase by all 13 models, with an average increase of 64% above the control proportion value of 0.12. The proportion of U.S. landfalling TCs is projected to increase for major hurricanes (+ 76% over control value of 0.077, increasing for 12 or 13 models, row labeled "mhur (cat 3–5)") and category 4–5 hurricanes (+ 350% over a control run value of 0.024, with 12 of 13 models increasing, row labeled "hur45").

To visually illustrate one of the more important findings in the table, Fig. 3 shows the tracks and intensities of the simulated U.S. landfalling hurricanes that are category 4 or 5 at landfall. The clear tendency for an increase in these very intense landfalling cases is seen across most of the different models, including

the CMIP3 and CMIP5 late 21st century ensemble ("CMIP3_ens18" and "CMIP5_LATE", respectively).

4. Summary And Conclusions

In this analysis, we explore future projection of U.S. landfalling TCs by examining a large number of cases generated using different climate model projections of large-scale environmental conditions, generally for the late 21st century under CMIP3 A1B scenario or the CMIP5 RCP4.5 scenario. We examined 13 different sets of projected warmed climate conditions based on 10 individual CMIP3 models or on the multi-model ensemble mean projection from the CMIP3 or CMIP5 models.

The most robust projections we simulate include an increase in the precipitation rate of U.S. landfalling TCs—a signal that increases in strength for the more intense categories of hurricanes, from + 18% averaged over all categories of TC (Cat 0–5) to almost + 200% for TCs that are Category 4 or 5 intensity at landfall. A robust reduction in TC frequency is projected for basin-wide counts (-25 to -45%) but this does not translate into a robust signal for U.S. landfalling TC frequency. Instead, a moderately significant and robust increasing signal emerges for the very intense U.S. landfalling TCs (category 4–5 storms). These average + 390% projected increase in frequency, with at least nominal increases projected for 10 of 13 models (with three of these projecting statistically significant increases) and no significant change for the remaining three models). Basin-wide PDI and duration are projected to decrease, while basin-wide intensity increases, but there is little significant signal in intensity projected for the U.S. landfalling TCs. Duration of TCs shows a significant decrease (averaging − 13%) while propagation speed shows a slight tendency to increase. The proportion of TCs that make U.S. landfall increases for almost all of the models, and the percentage increase in this proportion is especially large for the higher categories of TCs. It is this increase in proportion of U.S. landfalling TCs that contributes to an increase in the projected number of U.S. landfalling category 4–5 storms despite the projected decrease in overall numbers of TCs (including the weak decrease in basin-wide category 4–5 TCs in these projections).

Major caveats to our study include the limited skill shown by the downscaling framework in simulating the historical year-to-year variability of U.S. landfalling TC activity using SSTs and the NCEP/NCAR Reanalysis as large-scale climate forcings. There is also uncertainty in the climate change signal in the large-scale environmental parameters, which is partly reflected in the spread of results across the different model-derived scenarios. The spread shown in our results cannot be assumed to represent the true confidence intervals on the results in this study. Despite these limitations, it is important to test our models with such scenarios and continue to compare modeled scenarios with the growing observational database to work toward a better understanding of the changes in landfalling hurricane risk facing our society in the coming century.

5. Declarations

Acknowledgements. We thank the CMIP3 and CMIP5 modeling groups for contributing their simulations to the CMIP online archives.

6. References

1. Bender, M. A., I, Ginis, R. E. Tuleya, B. Thomas and T. Marchok, 2007: The operational GFDL coupled hurricane-ocean prediction system and a summary of its performance. *Mon. Wea. Rev.*, **135**(12).
2. Bender, M. A., T. R. Knutson, R. E.Tuleya, J. J.Sirutis, G. A.Vecchi, S. T. Garner, and I. M. Held, 2010: Modeled impact of anthropogenic warming on the frequency of intense Atlantic hurricanes. *Science*,**327**(5964), DOI:10.1126/science.1180568.
3. Bhatia, K.T., G. A. Vecchi, and T. R. Knutson, H. Murakami, J. Kossin, K. W. Dixon, and C. E. Whitlock, 2019: Recent increases in tropical cyclone intensification rates. *Nat.Commun.*,**10,** 635. https://doi.org/10.1038/s41467-019-08471-z
4. Colbert, A. J., B. J. Soden, G. A. Vecchi, G. A., and B. P. Kirtman, 2013: The Impact of Anthropogenic Climate Change on North Atlantic Tropical Cyclone Tracks, *Journal of Climate*, **26**(12), 4088-4095.
5. Dunstone, N., Smith, D., Booth, B. et al., 2013: Anthropogenic aerosol forcing of Atlantic tropical storms. *Nature Geosci.,***6,** 534–539. https://doi.org/10.1038/ngeo1854
6. Dwyer, J. G., S. J. Camargo, A. H. Sobel, M. Biasutti, K. A. Emanuel, G. A. Vecchi, M. Zhao, and M. K. Tippett, 2015: Projected twenty-first-century changes in the length of the tropical cyclone season. *J. Climate*, **28,** 6181–6192, https://doi.org/10.1175/JCLI-D-14-00686.1.
7. Goldenberg, S. B., C. W. Landsea, A. M. Mestas-Nunez, W. M. Gray, 2001: The Recent Increase in Atlantic Hurricane Activity: Causes and Implications. *Science,***293,** 474-479.
8. Hassanzadeh, P., C.-Y. Lee, E.Nabizadeh, et al., 2020: Effects of climate change on the movement of future landfalling Texas tropical cyclones. *Nat. Commun.***11,** 3319. https://doi.org/10.1038/s41467-020-17130-7Hill, K. A., and G. M.Lackmann, 2011: The impact of future climate change on TC intensity and structure: adownscaling approach, *J. Clim.*, **24**(17), 4644-4661.
9. Kalnay, E., and Coauthors, 1996: The NCEP/NCAR 40-Year Re-analysis Project. *Bull. Amer. Meteorol. Soc.,***77,** 437–471.
10. Klotzbach, P. J., et al., 2020: Surface pressure a more skillful predictor of normalized hurricane damage than maximum sustained wind. *Bull. Amer. Meteorol. Soc.*, **XX**, xx-xx-, doi:10.1175/BAMS-D-19-0062.1
11. Knutson, T., Camargo, S. J., Chan, J. C. L., Emanuel, K., Ho, C., Kossin, J., Mohapatra, M., Satoh, M., Sugi, M., Walsh, K., & Wu, L. (2020). Tropical cyclones and climate change assessment: Part II: Projected response to anthropogenic warming, *Bull. Amer. Meteorol. Soc.*, ***101***(3), E303-E322.
12. Knutson, T. R., J. J.Sirutis, S. T. Garner, I. M. Held, and R. E.Tuleya, 2007: Simulation of the recent multidecadalincrease of Atlantic hurricane activity using an 18-km-grid regional model. *Bull. Amer. Meteorol. Soc.,***88**(10), DOI:10.1175/BAMS-88-10-1549.
13. Knutson, T. R., J. J.Sirutis, G. A.Vecchi, S. T. Garner, M. Zhao, H.-S. Kim, M. A. Bender, R. E.Tuleya, I. M. Held, and G.Villarini, 2013: Dynamical downscaling projections of 21st century Atlantic hurricane activity: CMIP3 and CMIP5 model-based scenario. *J.Clim.*, **26**(17), DOI:10.1175/JCLI-D-12-00539.1.

14. Knutson, T., J. Sirutis, M. Zhao, R. Tuleya, M. Bender, G. Vecchi, G. Villarini, and D. Chavas, 2015: Global projections of intense tropical cyclone activity for the late 21st century from dynamical downscaling of CMIP5/RCP4.5 scenarios. *J.Clim.*, **28**(18), DOI:10.1175/JCLI-D-15-0129.1
15. Kossin, J.P., 2019: Reply to: Moon, I.-J. et al.; Lanzante, J. R.. *Nature***570,** E16–E22. https://doi.org/10.1038/s41586-019-1224-1.
16. Levin, E.L. and H. Murakami, 2019: Impact of Anthropogenic Climate Change on United States Major Hurricane Landfall Frequency . *J. Mar. Sci. Eng.***7**, 135.https://doi.org/10.3390/jmse7050135
17. Liu, M., G. A. Vecchi, J. A. Smith, and T. R. Knutson, 2019: Causes of large projected increases in hurricane precipitation rates with global warming. *npjClimAtmosSci***2,** 38 (2019). https://doi.org/10.1038/s41612-019-0095-3
18. Mann, M. E., and K. A. Emanuel, 2006: Atlantic hurricane trends linked to climate change, *Eos Trans. AGU*, 87(24), 233– 241, doi:10.1029/2006EO240001.
19. Murakami, H., T. L. Delworth, W. F. Cooke, M. Zhao, B. Xiang, P.-C. Hsu, 2020: Detected climatic change in global distribution of tropical cyclones. *Proc. Nat. Acad. Sci.*, **117** (20) 10706-10714; DOI: 10.1073/pnas.1922500117
20. Murakami, H., G. A. Vecchi, G. Villarini, T. L. Delworth, R. Gudgel, S. Underwood, X. Yang, W. Zhang, and S. Lin, 2016: Seasonal forecasts of major hurricanes and landfalling tropical cyclones using a high-resolution GFDL coupled climate model. *J. Climate*, **29,** 7977-7989.
21. Murakami, H., and B. Wang, 2010: Future Change of North Atlantic Tropical Cyclone Tracks: Projection by a 20-km-Mesh Global Atmospheric Model, *Journal of Climate*, **23**(10), 2699-2721.
22. Patricola, C.M., and M. F. Wehner, 2018:Anthropogenic influences on major tropical cyclone events. *Nature***563,** 339–346. https://doi.org/10.1038/s41586-018-0673-2
23. Pielke, R. A., Jr., J. Gratz, C. W. Landsea, D. Collins, M. A. Saunders, and R. Musulin, 2008: Normalized hurricane damage in the United States: 1900–2005. *Nat. Hazards Rev.,***9,** 29, https://doi.org/10.1061/(ASCE)1527-6988(2008)9:1(29).
24. Reed, K. A., M. F. Wehner, A. M. Stansfield, and C. M. Zarzycki, 2021: Anthropogenic influence on Hurricane Dorian's extreme rainfall. [in "Explaining Extremes of 2019 from a Climate Perspective"]. *Bull. Amer. Meteor. Soc.,* 102 (1), S9–S15, doi:https://doi.org/10.1175/BAMS-D-20-0160.1.
25. Tuleya, R. E., Bender, M., Knutson, T. R., Sirutis, J. J., Thomas, B., &Ginis, I. (2016). Impact of Upper-Tropospheric Temperature Anomalies and Vertical Wind Shear on Tropical Cyclone Evolution Using an Idealized Version of the Operational GFDL Hurricane Model, *Journal of the Atmospheric Sciences*, *73*(10), 3803-3820.
26. Tuleya, R, M. DeMaria, and R. J. Kuligowski, 2007: Evaluation of GFDL and simple statistical model rainfall forecasts for U.S. landfalling tropical storms. *Wea. Forecasting*, **22,** 56–70, doi:10.1175/WAF972.1.
27. Wright, D., T. R. Knutson, and J. A. Smith, 2015: Regional climate model projections of rainfall from U.S. landfalling tropical cyclones. *Climate Dynamics*, **45**(11-12), DOI:10.1007/s00382-015-2544-y.
28. Vecchi, G., T. Delworth, and B. Booth, 2017: Origins of Atlantic decadal swings. *Nature***548,** 284–285. https://doi.org/10.1038/nature23538
29. Vecchi, G. A., and T. R. Knutson, 2008: On estimates of historical North Atlantic tropical cyclone activity. *J.Clim.*, **21**(14), DOI:10.1175/2008JCLI2178.1.
30. Vecchi, G. A., and T. R. Knutson, 2011: Estimating annual numbers of Atlantic hurricanes missing from the HURDAT database (1878-1965) using ship track density. *J.Clim.*, **24**(6), DOI:10.1175/2010JCLI3810.1.
31. Vecchi, G. A., C. Landsea, W. Zhang, G. Villarini, and T. R. Knutson, 2021: **Changes in Atlantic major hurricane frequency since the late-19th century**. *Nature Communications*, **12**, 4054, DOI:10.1038/s41467-021-24268-5.
32. Yablonsky, R. M., I. Ginis, B. Thomas, V.Tallapragada, D. Sheinin, and L.Bernardet, 2015:Description and Analysis of the Ocean Component of NOAA's Operational Hurricane Weather Research and Forecasting Model (HWRF), Journal of Atmospheric and Oceanic Technology, 32(1), 144-163.
33. Yan, X., R. Zhang, and T. R. Knutson, 2017: The role of Atlantic overturning circulation in the recent decline of Atlantic major hurricane frequency. *Nat. Commun***. 8,** 1695. https://doi.org/10.1038/s41467-017-01377-8
34. Zhang, G., H. Murakami, T. R. Knutson, R. Mizuta, and K. Yoshida, 2020: **Tropical cyclone motion in a changing climate.***Science Advances*, **6(17)**, eaaz7610, DOI:10.1126/sciadv.aaz7610.
35. Zhang, R., Delworth, T. L., Sutton, R., Hodson, D. L. R., Dixon, K. W., Held, I. M., Kushnir, Y., Marshall, J., Ming, Y., Msadek, R., Robson, J., Rosati, A. J., Ting, M., &Vecchi, G. A., 2013: Have Aerosols Caused the Observed Atlantic Multidecadal Variability?, *Journal of the Atmospheric Sciences*, *70*(4), 1135-1144.

7. Table

Table 1. Summary projections for various Atlantic basin or U.S. landfallingTC metrics. Underlined bold text indicates values that are statistically significant at the 0.05 level. Column A (Control) refers to the control run values of the TC metrics, derived from downscaling NCEP Reanalyses (1981-2006). Remaining columns (B-N) refer to percent changes in the TC metric for the given climate change scenario or model, as identified in the "Key to columns" below. The final column ("Average") shows the average of the percent changes in columns B-N, with the value in parentheses indicating the number of models that simulated the same sign change as the average change. "lf" = landfalling storms over the contiguous U.S.; TS (cat 0) = frequency (annual number of storms) of tropical storm-strength (sub-hurricane strength); H1…H5 = frequency of category 1…5 hurricanes; all_TC(cat 0-5) = frequency of all tropical storms and hurricanes combined; hur (cat 1-5) = frequency of all hurricanes (category 1-5); mhur (cat 3-5) = frequency of major hurricanes of category 3-5; hur45 = frequency of category 4 & 5 hurricanes; lf_TS (cat 0) = frequency of U.S. landfalling sub-hurricane strength storms; lf_all_TC(cat 0-5) = frequency of all U.S. landfalling tropical storms and hurricanes; lf_maxwnd_ts = average maximum wind intensity at landfall of U.S. landfalling tropical storms and hurricanes; PDI = power dissipation index in units of 10^9 m^3 s^{-2}; max_wind_all_TC= average lifetime maximum surface wind speed for all tropical storms and hurricanescombined (m s^{-1}); duration = storm accumulated lifetime with at least tropical storm strength (days); trans speed = average propagation speed of storm (m s^{-1}); rain_all_TC (cat 0-5) = average rain rate within 100 km of storm center of all tropical storms and hurricanes at time of maximum intensity (mm day^{-1}); lf_rain_all_TC(0-5) = average rain rate within 100 km of storm center of all tropical storms and hurricanes at time of U.S. landfall (mm day^{-1}). For U.S. landfall proportions, the

control values and percent changes are for the fraction of storms of a given category or range of categories that make U.S. landfall. The U.S. landfall proportion is calculatedas the ratio of all U.S. landfalling storms to the sum of all landfalling and non-landfalling storms, with storm counts accumulated over all seasons prior to computing the ratio.Statistical significance tests, typically done in the Table by comparing across individual seasons for a given model, were not performed for the U.S. landfall proportions.

Key to columns in table.

A	Control	H	CMIP3_mri
B	CMIP3_ens18	I	CMIP3_gfdl-cm20
C	CMIP5_EARLY	J	CMIP3_hadgem1
D	CMIP5_LATE	K	CMIP3_miroc-hi
E	CMIP3_gfdl_cm2	L	CMIP3_ccsm3
F	CMIP3_mpi	M	CMIP3_ingv
G	CMIP3_hadcm3	N	CMIP3_miroc-med

Table 1. Summary Results.

METRIC:	A. Control	Model B	(% C	Change) D	E	F	G	H	I	J	K	L	M	N	Av
TS (cat 0)	2.704	-9.6	-2.7	2.7	-9.6	-8.2	-8.2	-16.5	0.0	**-30.1**	4.1	-13.7	-12.4	-28.8	-1 (1
H1	2.37	**-45.3**	-26.5	**-45.3**	-35.9	**-39.1**	**-59.4**	-28.1	-32.8	**-54.7**	**-56.2**	-32.8	-34.3	**-51.6**	-4
H2	1.852	**-56.0**	-10.0	-36.0	**-48.0**	**-52.0**	**-68.0**	**-58.0**	-10.0	**-62.0**	**-60.0**	-18.0	**-50.0**	**-62.0**	-4 (1
H3	2.296	-25.8	**-37.1**	**-33.8**	-24.2	**-58.1**	**-75.8**	-22.6	-17.7	**-79.1**	**-62.9**	-27.4	**-38.7**	**-61.3**	-4 (1
H4	1.37	10.9	-8.1	2.7	24.4	-27.0	**-62.1**	0.0	64.9	**-81.1**	-18.9	0.0	-2.7	-24.3	-9
H5	0.185	80.0	-40.0	120.0	**280.5**	80.0	20.0	120.0	**360.5**	-80.0	20.0	20.0	180.5	80.0	95
all_TC (cat 0-5)	10.778	**-24.7**	-17.9	-20.3	-15.8	**-34.0**	**-50.5**	**-23.0**	1.7	**-58.8**	**-37.1**	-19.2	**-24.7**	**-44.0**	-2 (1
hur (cat 1-5)	8.074	**-29.8**	-22.9	**-28.0**	-17.9	**-42.7**	**-64.7**	**-25.2**	2.3	**-68.3**	**-50.9**	-21.1	**-28.9**	**-49.1**	-3 (1
mhur (cat 3-5)	3.852	-7.7	-26.9	-13.5	7.7	**-40.4**	**-66.4**	-7.7	29.8	**-79.8**	**-43.3**	-15.4	-15.4	**-41.4**	-2 (1
hur45	1.556	19.0	-12.0	16.6	54.7	-14.3	**-52.4**	14.3	**99.9**	**-81.0**	-14.3	2.4	19.0	-12.0	3.
lf_TS (cat 0)	0.815	-22.7	-9.1	40.9	4.5	13.6	36.3	0.0	22.7	4.5	-22.7	9.1	54.5	-18.2	8.
lf_H1	0.444	-16.7	25.2	16.9	-8.3	-33.3	-66.7	25.2	41.9	-41.7	-8.3	91.9	0.0	-33.3	-0
lf_H2	0.259	-28.6	114.7	28.6	14.3	-57.1	-42.9	0.0	28.6	-42.9	-14.3	14.3	28.6	-42.9	0.
lf_H3	0.259	-57.1	42.9	-57.1	28.6	-14.3	-71.4	-42.9	85.7	-71.4	-28.6	-14.3	42.9	-42.9	-1
lf_H4	0.037	300.0	100.0	800.0	**700.0**	0.0	200.0	500.0	**1200.0**	0.0	0.0	0.0	300.0	100.0	32
lf_all_TC (cat 0-5)	1.815	-20.4	26.5	34.7	28.5	-10.2	-10.2	12.2	**63.3**	-24.5	-18.4	26.5	42.9	-26.6	9.
lf_hur (cat 1-5)	1	-18.5	55.6	29.6	48.1	-29.6	**-48.1**	22.2	**96.3**	-48.1	-14.8	40.7	33.3	-33.3	1(
lf_mhur (cat 3-5)	0.296	-12.5	50.0	50.0	**162.8**	0.0	-25.0	37.5	**237.8**	-62.5	-25.0	-12.5	87.8	-25.0	35
lf_hur45	0.037	300.0	100.0	**800.0**	**1100.0**	100.0	300.0	600.0	**1302.7**	0.0	0.0	0.0	400.0	100.0	39
lf_maxwnd_all_TC	36.364	-4.0	0.6	-3.3	4.8	-11.3	**-13.0**	-3.4	10.6	**-15.4**	-9.0	-5.3	-1.2	-3.9	-4
lf_maxwnd_hur	45.944	-0.6	-3.7	5.8	**13.6**	3.2	3.5	3.0	11.1	-2.6	-2.5	-5.5	5.3	-0.8	2.

PDI	381.994	-14.0	**-29.0**	-19.1	1.3	**-36.0**	**-65.5**	-20.7	22.1	**-80.5**	**-43.1**	-12.5	-20.0	**-43.4**	-27.7 (11)
max_wind_all_TC	**43.367**	3.5	-1.4	0.7	7.3	-2.8	**-10.8**	3.6	8.9	**-12.7**	-5.1	1.2	3.3	2.2	-0.2 (5)
max_wind_hur	**49.417**	**8.1**	1.2	**6.0**	**9.7**	4.1	1.4	**5.7**	**10.4**	**-6.9**	6.0	3.4	**6.2**	6.4	4.7 (12)
duration	7.367	-7.1	**-12.1**	-9.1	**-9.9**	**-16.1**	**-28.7**	**-8.9**	-8.8	**-28.1**	**-25.0**	1.3	-8.7	**-12.2**	-13.3 (12)
trans_speed	5.658	3.1	-1.7	2.9	**12.8**	2.8	-2.1	0.5	**10.1**	3.8	3.6	3.7	1.5	-2.5	3.0 (10)
rain_all_TC (cat 0-5)	163.2	**24.7**	10.9	**19.5**	**32.8**	21.3	13.8	**21.1**	**29.0**	-9.2	27.5	**14.4**	**18.9**	18.1	18.7 (12)
rain_hur (cat 1-5)	234.252	**23.9**	**10.6**	**23.3**	**29.4**	**24.2**	28.7	**25.8**	**28.7**	1.7	**29.1**	**10.2**	**20.7**	**25.8**	21.7 (13)
rain_mhur (cat 3-5)	341.269	**19.9**	**12.9**	**20.9**	**24.0**	**14.2**	20.3	**21.2**	**25.3**	12.1	21.6	**14.8**	**15.4**	**22.1**	18.8 (13)
rain_hur45	421.257	**24.8**	15.7	**21.9**	**24.3**	7.4	20.0	**22.1**	**20.9**	14.9	25.5	16.5	**17.6**	24.6	19.7 (13)
lf_rain_all_TC (0-5)	169.65	14.5	13.6	24.9	**40.4**	34.3	-4.3	31.5	**43.5**	-11.4	8.1	8.5	19.6	16.2	18.4 (11)
lf_rain_hur (1-5)	223.406	13.9	7.2	**29.3**	**55.2**	44.6	25.4	29.1	**41.7**	8.0	21.4	8.2	31.5	20.0	25.8 (13)
lf_rain_mhur (cat 3-5)	279.786	45.3	6.2	46.8	**51.7**	52.5	36.4	35.7	**38.9**	28.7	24.6	13.5	42.6	55.3	36.8 (13)
Table 1 (contd.)	160.66	204.1	52.8	**165.4**	**213.5**	229.2	238.8	**183.4**	**191.9**	157.1	279.5	152.9	**254.0**	186.6	193 (13)
lf_rain_hur45															
US Landfall proportions															
TS (cat 0)	0.301	-14.5	-6.5	37.1	15.7	23.8	48.6	19.7	22.7	49.6	-25.7	26.4	76.2	14.9	22.2 (10)
H1	0.187	52.4	70.5	113.8	43.0	9.4	-18.0	74.2	111.1	28.7	109.5	185.5	52.3	37.6	66.9 (12)
H2	0.140	62.3	138.5	100.9	119.8	-10.7	78.5	138.0	42.8	50.3	114.2	39.3	157.1	50.3	83.2 (12)
H3	0.113	-42.3	127.1	-35.2	69.6	104.4	18.0	-26.2	125.7	36.4	92.5	18.1	133.1	47.6	51.4 (10)
H4	0.027	260.8	117.6	776.3	543.2	37.0	691.9	500.0	688.4	429.0	23.3	0.0	311.1	164.2	349 (12)
all_TC (cat 0-5)	0.168	5.7	54.0	68.9	52.7	36.1	81.5	45.8	60.5	83.1	29.8	56.6	89.8	31.1	53.5 (13)
hur (cat 1-5)	0.124	16.1	101.9	79.9	80.4	22.8	46.9	63.4	91.9	63.9	73.6	78.3	87.5	31.0	64.4 (13)
mhur (cat 3-5)	0.077	-5.2	105.3	73.4	144.1	67.8	122.9	48.9	160.3	85.7	32.2	3.4	122.0	27.9	76.0 (12)
hur45	0.024	236.1	127.2	671.6	675.7	133.5	739.9	512.6	601.6	425.7	16.7	-2.3	320.1	127.2	353 (12)

Figures

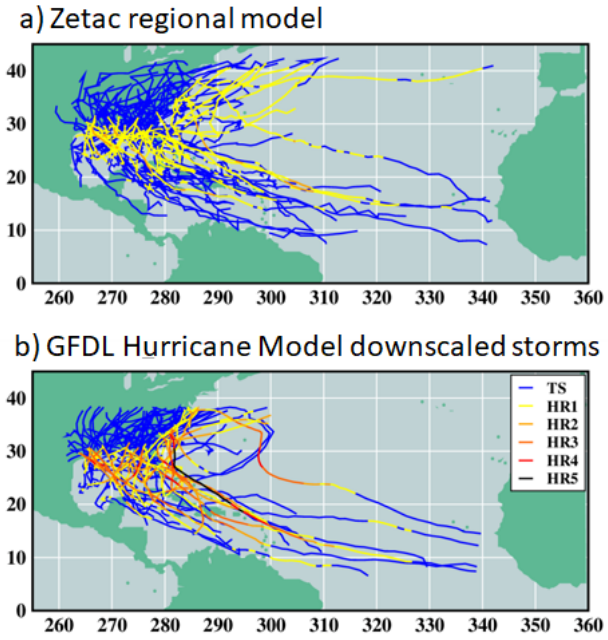

Figure 1

U.S. landfalling tropical storms and hurricanes for the years 1980-2013 as simulated by: a) the Zetac regional model based on initial conditions, boundary conditions, and large-scale interior spectral nudging targets derived from the NCAR/NCEP Reanalyses for Aug.-Oct. seasons; and b) the GFDL hurricane model using all tropical storm cases from the Zetac regional model (both landfalling and non-landfalling cases in Zetac) as initial conditions and boundary conditions for higher-resolution downscaled simulations, but plotting only contiguous U.S. landfalling hurricane model cases.

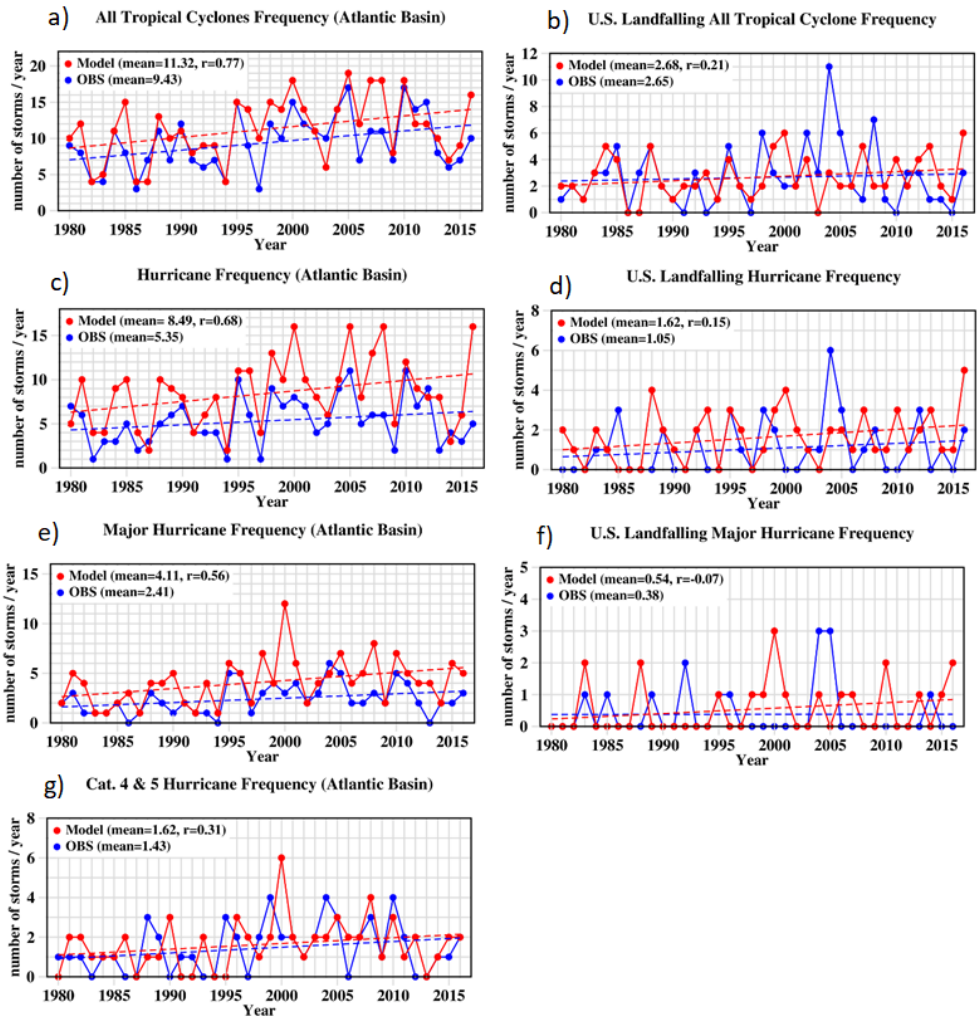

Figure 2

Annual (Aug.-Oct.) counts of Atlantic basin-wide (a, c, e, g) and contiguous U.S. landfalling (b, d, f) tropical cyclones in observations (blue) or as simulated in the downscaling framework using NCEP Reanalysis large-scale forcing. Intensity categories are: a,b) tropical storm and higher; c,d) Category 1-5 hurricanes; e,f) Major (Category 3-5) hurricanes; or g) very intense (Category 4-5) hurricanes. The series means and correlations (r) between observed and modeled series are shown in each panel. Dashed lines are linear trends. Differing y-axis scaling is used.

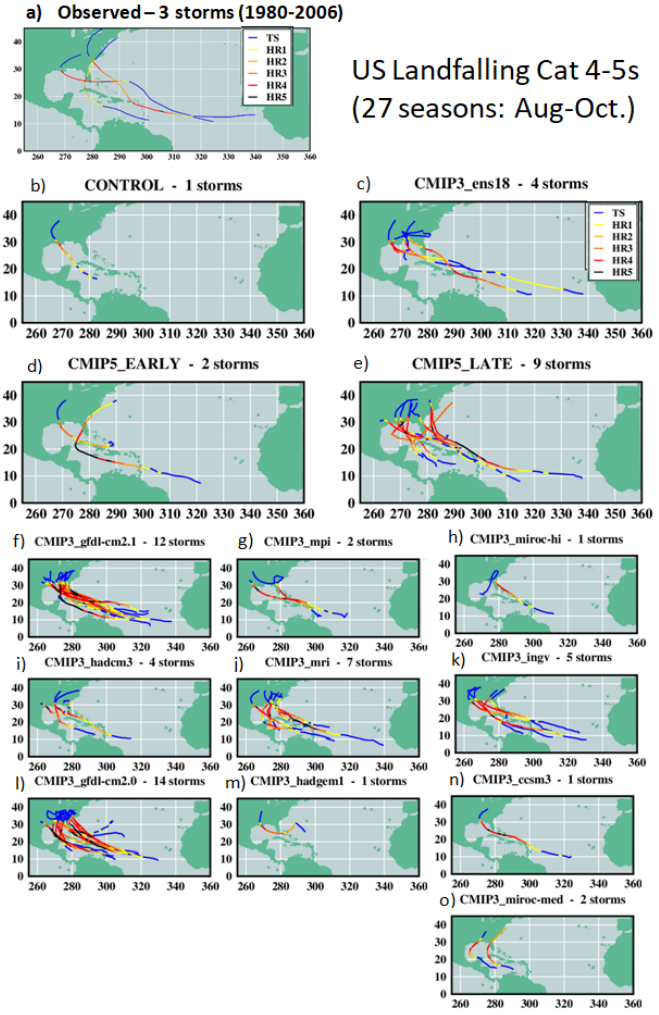

Figure 3

Tracks of all tropical cyclones that made U.S. landfall while at Category 4 or 5 intensity based on:a) observations or b) NCEP Reanalysis-driven present-day simulations (Control) for Aug-Oct. of the years 1980-2006. The remaining simulation panels used the reanalysis variability from 1980-2006 while their mean climate conditions were altered from the reanalysis according to warming scenarios derived from:c) CMIP3 18-model ensemble (late 21st century A1B scenario);d, e) CMIP5 multi-model ensemble early (d) and late (e) 21st century RCP4.5scenarios; or f-o) individual CMIP3 models. See text for details.